Available online at www.sciencedirect.com
SCIENCE DIRECT
Journal of Molecular Catalysis A: Chemical 242 (2005) 1–17
JOURNAL OF MOLECULAR CATALYSIS A: CHEMICAL
www.elsevier.com/locate/molcata

Kinetic and binding studies of the thiolate–cobalt tetrasulfophthalocyanine anaerobic reaction as a subset of the Merox process

Eduard M. Tyapochkin, Evguenii I. Kozliak *

Department of Chemistry, University of North Dakota, 2nd Avenue North & Cornell, Grand Forks, ND 58202, USA

Received 14 April 2005; received in revised form 1 July 2005; accepted 2 July 2005
Available online 24 August 2005

Abstract

Binding and kinetic studies of the complexation of thiolates/thioacid salts with 4,4′,4″,4‴-cobalt tetrasulfophthalocyanine (Co^{II}TSPc) in aqueous solutions were conducted using UV–vis spectrophotometry under anaerobic conditions. Stepwise binding of two thiolate equivalents by one CoTSPc equivalent was observed. One-to-one thiolate binding constants increase along with thiolate basicity and drop when the ligand's pK_a is less than 3.5. Binding constants for the second thiolate molecule are nearly one-order of magnitude smaller than those for the first one, and their dependence on thiolate basicity is less pronounced. Two-to-one thiolate binding occurs only if the resulting complex is oligomeric (as for the original Co^{II}TSPc in aqueous media) and is accompanied by greater Co^{II}–Co^{I} reduction. Significant steric effects observed in 2:1 thiolate–CoTSPc binding indicate ligand–ligand interactions in stacked dimers (oligomers). Based on kinetic curves, thiolate binding appears to be a multi-step process with lag periods prior to the axial binding of both the first and second ligands, thus pointing to intermediate formation of outer-sphere complexes. Evidence was obtained that the rate-limiting step is electron transfer from sulfur to cobalt. The values of reciprocal Michaelis constants for the Merox process (CoTSPc-catalyzed aerobic autoxidation of the same substrates) are similar to those of the anaerobic 2:1 binding constants, thus indicating quasiequilibrium and the significance of dithiolate cobalt phthalocyanine complexes in catalysis.

Keywords: Cobalt tetrasulfophthalocyanine; Merox process; Thiolate autoxidation

1. Introduction

Autoxidation of basic thiolates catalyzed by cobalt phthalocyanines, e.g., 4,4′,4″,4‴-cobalt tetrasulfophthalocyanine (Co^{II}TSPc), is one of the primary methods used in the deodoration of petroleum products (Merox process, Reaction 1) [1]:

$$2H_2O + 4RS^- + O_2 \xrightarrow{CoTSPc} 2RSSR + 4OH^- \quad (1)$$

Cobalt phthalocyanine catalyzed autoxidation of low-basicity thiolates is also used for commercial scale syntheses of disulfides and for improving the efficiency of metal ore refining using the flotation method, by controlled partial oxidation of thioacid salts to bis-thiocarboxylates (for generality, also called "disulfides" henceforth) [2–6].

As has been suggested, the general mechanism for this reaction includes the formation of a CoTSPc–thiolate complex, which then reacts with oxygen, forming an unstable ternary thiolate–CoTSPc–oxygen intermediate. The ternary complex rapidly decomposes to yield the products (Scheme 1) [1,7–14].

However, many important details of this mechanism are yet to be elucidated. For example, little is known about the role of the aggregation of Co^{II}TSPc or its reduced forms in the catalysis of Reaction 1, although there have been indications that the phthalocyanine dimers (oligomers) are more reactive than monomers [8–14]. The formation of Co^{II}TSPc dimers in aqueous solutions, which depends on ionic strength, was documented earlier [15–22]. However, the postulated formation of stacked aggregates greater than

* Corresponding author. Tel.: +1 70 17 772145; fax: +1 70 17 772331.
E-mail address: ekozliak@mail.chem.und.nodak.edu (E.I. Kozliak).

1381-1169/$ – see front matter © 2005 Elsevier B.V. All rights reserved.
doi:10.1016/j.molcata.2005.07.008

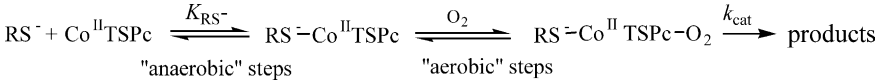

Scheme 1.

dimers at high ionic strength (>0.01 M) has not been quantified. In addition, aggregation was thoroughly investigated only for Co^{II}TSPc but not for its thiolate complexes. Another poorly explored topic is the potential involvement of the second thiolate molecule in the formation of the ternary RS^-–CoTSPc–O_2 complex in Scheme 1, as some studies have indicated [10,23–28].

A common difficulty in studying the mechanism of Reaction 1 is isolation and characterization of Merox process intermediates. Attempts to concentrate thiolate complexes by either evaporation or addition of organic solvents may result in changing their composition and aggregation state. This problem severely limits the choice of applicable methods. Application of ^{1}H NMR to diamagnetic metal sulfonated phthalocyanines in aqueous solutions yields broadened and non-informative lines due to their aggregation [29]; the paramagnetic Co^{II}TSPc yields even less informative spectra. In turn, ESR is not applicable because of strong Co^{II}TSPc association in aqueous solutions leading to radical coupling [30,31]. Mass spectrometry of metal tetrasulfophthalocyanines and other high molecular mass chemicals can be used only in low-ionic strength solutions (containing organic solvents) to minimize ion signal suppression [29,32,33]. IR generally could not be used in aqueous solutions because of strong background absorption.

Earlier, using binding and kinetic studies (along with the UV–vis spectrophotometry), we investigated interactions of Co^{II}TSPc with thiolates under anaerobic conditions, as a subset of Reaction 1, in both non-aqueous media [34] and aqueous solutions [35,36]. We obtained evidence for hydrophobic effects as well as the pronounced influence of the thiolate basicity on Merox process kinetics, and showed that the variations in values of CoTSPc–thiolate binding constants are due to both of these effects [35,36]. We also demonstrated that the main features of the anaerobic process are qualitatively similar for a wide range of non-aromatic thiolates of varied basicity, including thioacid salts [34–36]. (Hereafter, we will not distinguish between the thiolates and thioacid salts calling them just “thiolates” unless otherwise stated.) For instance, all of the thiolates reacting with Co^{II}TSPc in aqueous solutions under anaerobic conditions (Reaction 2) could not completely reduce cobalt, so its oxidation number in the resulting oligomeric thiolate–phthalocyanine complexes is between +1 and +2 [35,36].

$$RS^- + Co^{II}TSPc \overset{K_{RS^-}}{\rightleftharpoons} RS^-–Co^{II}TSPc \leftrightarrow RS^\bullet–Co^{I}TSPc \quad (2)$$

Using thiolates of low basicity as substrates allowed us to reduce the reaction rate [36]. For common basic alkyl thiolates, the bulk of the process takes only seconds for completion, thus making it difficult to obtain full kinetic curves [10]. In turn, obtaining full kinetic curves allowed us to observe otherwise hidden kinetic features. Upon the discrimination of other possible mechanisms, the kinetic scheme was suggested [36]. This scheme is separated within a box in Fig. 1.

This paper presents the results of comprehensive binding and kinetic studies of anaerobic Reaction 2 (using UV–vis spectrophotometry), for a wide basicity range of thiolates, while connecting it to aerobic Reaction 1. To keep the CoTSPc aggregation consistent, despite the presence of varied high thiolate concentrations, the study was conducted at a high and constant ionic strength (0.6 M). The most important new observation is the binding of the second thiolate molecule to CoTSPc (2:1 binding). This occurrence and other contributions (thermodynamic and kinetic effects of the thiolate basicity and hydrophobicity, separation of binding and reduction equilibrium constants for Reaction 2, and a discovery of a slow final step) resulted in the adjustment of the original kinetic scheme and calculation of its key constants.

2. Experimental

2.1. Materials

4,4′,4″,4‴-CoTSPc was provided by Dr. T.P.M. Beelen (Eindhoven Technology University, The Netherlands). Sodium monothiophosphate (Na_3PO_3S), the potassium salt of *O*-ethylxanthic acid (EtOCSSK), sodium diethyldithiophosphate [$(EtO)_2PSSNa$], potassium trithiocarbonate (K_2CS_3), sodium diethyldithiocarbamate ($Et_2NCSSNa$), potassium thioacetate (CH_3COSK), DL-cysteine (Cys) and 2-mercaptoethanol (HOC_2H_4SH) were purchased as pure reagent-grade chemicals. Alkyl xanthogenates were synthesized as previously described [36]. Thioacid salts were additionally purified by dissolving them in hot ethanol or acetone and then precipitating by slow addition of the filtered solution into toluene. In a second purification step conducted similarly, petroleum ether was used as the precipitating agent instead of toluene. Purified thiolates were dried to a constant weight under vacuum in a dessicator containing KOH pellets and then stored in the same dessicator under dry nitrogen. Fresh thiolate solutions were prepared under nitrogen prior to each experiment. Custom-made anaerobic cells [23] for binding and kinetic studies of Reaction 2 were manufactured using Starna Inc. glassware.

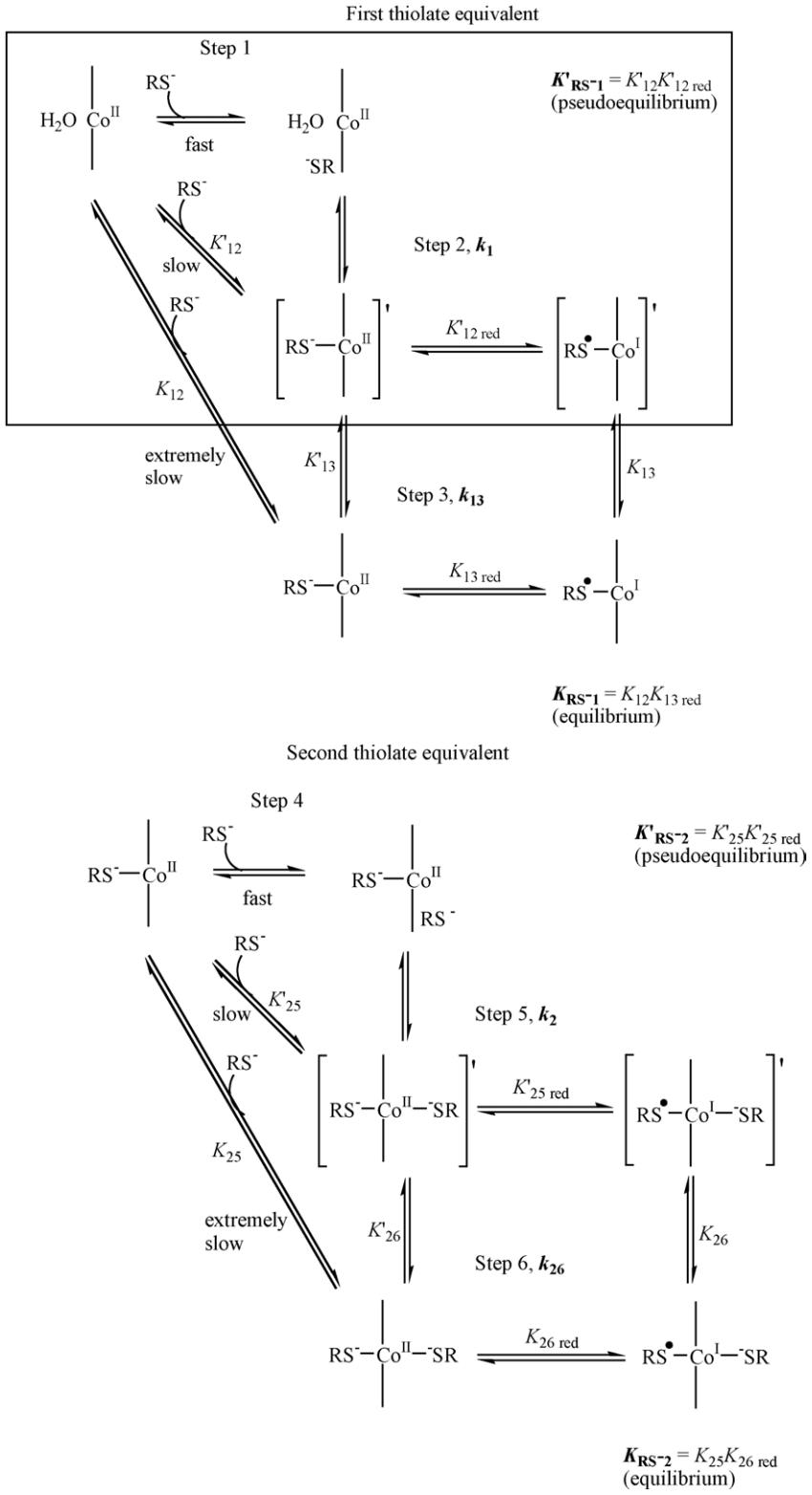

Fig. 1. CoTSPc–thiolate reactions in aqueous solutions involving the first and second thiolate equivalents. Equilibrium and kinetic constants obtained directly from the experiments are marked in boldface, whereas equilibrium constants determined indirectly are shown in plain font. Constants obtained at pseudoequilibrium (prior to extremely slow Steps 3 and 6) and the corresponding intermediates are marked with primes. For equilibrium and kinetic constants, the first digit in the subscript refers to the stoichiometry of binding (1 for 1:1 binding, and 2 for 2:1 binding), whereas the second digit denotes the corresponding step in this figure. The scheme suggested earlier [36] is shown within the box. For the reader's convenience, the pertinent portions of this figure are shown in the beginning of the sections in Section 3 that discuss the corresponding reactions and their equilibrium/kinetic constant values.

2.2. Methods

2.2.1. General experimental methods

The pK_a values of the thiolate conjugate acids were determined by acid titration. The study was conducted in aqueous solutions with the ionic strength adjusted to 0.60 M by addition of sodium perchlorate at $20.0 \pm 0.1\,^{\circ}C$ (thermostat-controlled). Titration was done using an HCl titrant and a micropipette. Absorption peaks of the thiolates at 200–290 nm were monitored using a Shimadzu UV-2501PC spectrophotometer. Technical details of the pK_a determination have been described previously [36]. It is of note that all pK_a values considered in this study pertain to the conjugate acids of thiolates; however, for the sake of simplicity, we will call them "thiolate pK_as" henceforth.

All binding and kinetic studies were performed at $20.0 \pm 0.1\,^{\circ}C$ in aqueous solutions. A 0.15 M borate buffer (pH 10.5) with the ionic strength adjusted to 0.60 M with sodium perchlorate was used in all cases except for experiments using DL-cysteine. Sodium perchlorate was chosen because it does not coordinate to CoTSPc. Experiments with DL-cysteine were conducted at its optimal pH 9.5 [7]. The concentration of CoTSPc was 1.0×10^{-5} M unless otherwise indicated; thiolate concentrations were at least one order of magnitude larger, in the range of 5.0×10^{-4} to 5.0×10^{-1} M. Spectra of the CoTSPc–thiolate complexes were recorded on a Shimadzu UV-2501PC spectrophotometer after mixing the degassed reagent solutions under anaerobic conditions (10^{-2} Torr vacuum). The degassing of solutions was achieved using three freeze-pump-thaw cycles. The achievement of equilibrium was assessed by recording no further detectable change in absorbance at 626 and 450 nm over a period of 24 h. It usually occurred in 5–7 days from the start of the experiment.

The 626-nm absorption peak was used for monitoring the reagent (Co^{II}TSPc) concentration in kinetic studies of Reaction 2. Kinetic experiments of Reaction 1 (measuring its overall rate) were conducted at $20.0 \pm 0.1\,^{\circ}C$ using an Instech dissolved oxygen-measuring system with a Clark electrode [35–38]. The concentrations of CoTSPc and oxygen were 1.0×10^{-5} and $(2.0 \pm 0.1) \times 10^{-4}$ M, respectively. Oxygen concentrations were adjusted by time-controlled saturation of the thiolate solutions with nitrogen. Thiolate concentrations ranged from 1.0×10^{-3} to 5.0×10^{-1} M. Autoxidation rates of thiolates were measured with and without CoTSPc, and the overall rate of Reaction 1 was calculated by subtracting the rate of the non-catalyzed reaction from that in the presence of CoTSPc.

To validate the formation of intermediates, singular value decomposition analysis (SVD) was performed on kinetic data using a free trial version of SPECFIT program.

Statistical treatment of data was performed using standard methods [39]; the errors were determined as standard deviations. For parameters calculated from double-reciprocal plots, experimental errors (standard deviations) were determined using linear regression statistical analysis (Origin software).

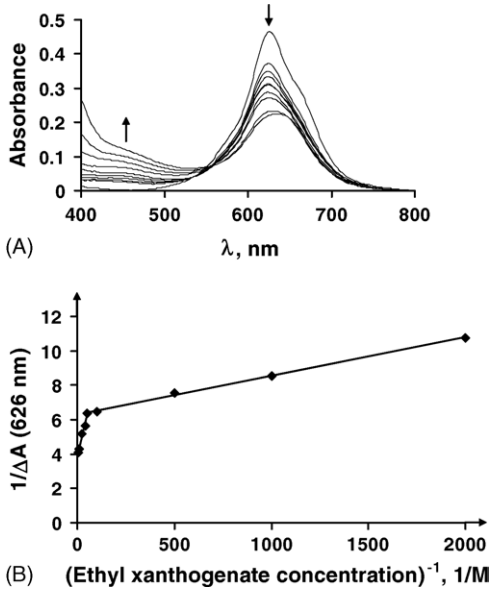

Fig. 2. (A) UV–vis spectra of 1.0×10^{-5} M CoTSPc with increasing ethyl xanthogenate concentrations at equilibrium. Concentrations of ethyl xanthogenate were 0, 5.0×10^{-4}, 1.0×10^{-3}, 2.0×10^{-3}, 1.0×10^{-2}, 2.0×10^{-2}, 2.5×10^{-2}, 4.0×10^{-2}, 1.0×10^{-1}, 2.0×10^{-1} M. The arrows indicate absorbance changes upon increase in ethyl xanthogenate concentration. Borate buffer (0.15 M), pH 10.5, ionic strength 0.60 M, under anaerobic conditions. (B) Double-reciprocal plot based on data from (A). ΔA is the difference between the absorbance at 626 nm of the initial Co^{II}TSPc and that at a given concentration of ethyl xanthogenate.

2.2.2. Binding constant determination

To determine the CoTSPc–thiolate binding constants, $K_{RS\text{-}1}$ and $K_{RS\text{-}2}$, the UV–vis spectra were recorded at equilibrium while varying the thiolate concentrations within a range of 5.0×10^{-4} to 1.0×10^{-2} M for $K_{RS\text{-}1}$ and 2.0×10^{-2} to 5.0×10^{-1} M for $K_{RS\text{-}2}$, respectively (as shown in Figs. 2A and 3). Then, the difference between the absorbance of the

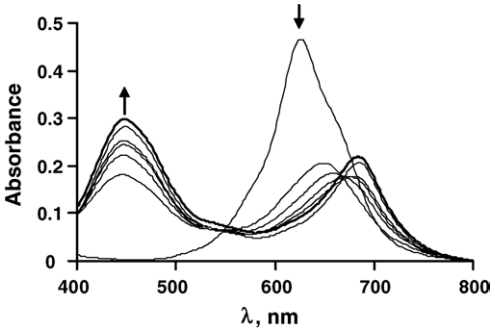

Fig. 3. UV–vis spectra of 1.0×10^{-5} M CoTSPc with increasing 2-mercaptoethanol concentrations at equilibrium. Concentrations of 2-mercaptoethanol were 0, 2.5×10^{-2}, 5.0×10^{-2}, 1.0×10^{-1}, 2.5×10^{-1}, and 5.0×10^{-1} M (the bold line represents the CoTSPc spectrum with 0.10 M $NaBH_4$). The arrows indicate absorbance changes upon increase in 2-mercaptoethanol concentration. Borate buffer (0.15 M), pH 10.5, ionic strength 0.60 M, under anaerobic conditions.

CoTSPc–thiolate complex and that of the original Co^{II}TSPc at 626 nm (ΔA_{626}) was plotted as a double-reciprocal plot versus the thiolate concentration (Fig. 2B). A detailed derivation for determining binding constants using this method has been reported previously [35].

Cobalt reduction constants, $K_{13\,red}$ and $K_{26\,red}$ (Fig. 1), were determined by combining the corresponding equilibrium constant expressions: $K_{13\,red}$ ($K_{26\,red}$) = $[Co^{I}TSPc]_{eq}/[Co^{II}TSPc]_{eq}$, and the mass balance equation $[Co^{I}TSPc]_{eq} + [Co^{II}TSPc]_{eq} = [CoTSPc]_0$: $K_{13\,red}$ ($K_{26\,red}$) = $x/(1-x)$, where x is the fraction of the reduced form, $[Co^{I}TSPc]_{eq}/[CoTSPc]_0$. The $[Co^{I}TSPc]_{eq}/[CoTSPc]_0$ ratio was determined by recording the equilibrium absorbance of the complex at 450 nm and taking A_{450} of the "pure" Co^{I}TSPc, obtained by the reaction of CoTSPc with 0.1 M sodium borohydride in the same buffer, as a reference for the complete (100%) reduction. The other key constants for the reaction scheme shown in Fig. 1, K_{12} and K_{25}, were calculated using detailed balance considerations, $K_{RS\text{-}1} = K_{12}K_{13\,red}$ and $K_{RS\text{-}2} = K_{25}K_{26\,red}$.

The other set of experimental binding constants, $K'_{RS\text{-}1}$ and $K'_{RS\text{-}2}$, was determined at pseudoequilibrium, prior to an extremely slow final step in the kinetic curve (see Section 3.2). The primes (K') will denote pseudoequilibrium constants henceforth. These binding constants, as well as the analogs of the cobalt reduction constants, $K'_{12\,red}$ and $K'_{25\,red}$, were determined in a similar way as those at equilibrium. The binding constants corresponding to K_{12} and K_{25}, K'_{12} and K'_{25}, were obtained using the following equations valid at pseudoequilibrium: $K'_{RS\text{-}1} = K'_{12}K'_{12\,red}$ and $K'_{RS\text{-}2} = K'_{25}K'_{25\,red}$. Finally, equilibrium constants K'_{13} and K'_{26} and K_{13} and K_{26} (Fig. 1) were calculated using the detailed balance considerations: $K_{12} = K'_{12}K'_{13}$; $K_{25} = K'_{25}K'_{26}$ and $K_{13} = K'_{13}K_{13\,red}/K'_{12\,red}$; $K_{26} = K'_{26}K_{26\,red}/K'_{25\,red}$.

3. Results and discussion

3.1. Binding studies

3.1.1. First thiolate equivalent: separation of CoTSPc binding and reduction

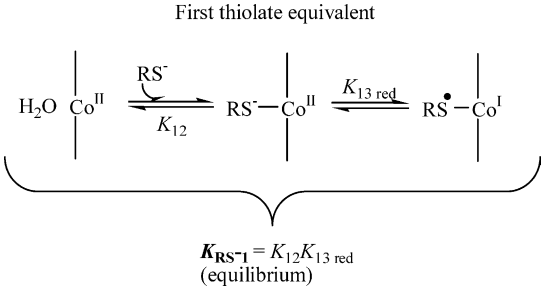

Spectral changes that occur in the reaction of CoTSPc with low-basicity thiolates at low concentrations under anaerobic conditions were as described earlier: the absorbance of the aggregated Co^{II}TSPc at 626 nm decreased in time with concomitant formation of a low-intensity, broad band at 635 nm and another band at 450 nm, until the equilibrium value was reached (Fig. 2A [25,35,36,40–43]). The final spectrum did not change anymore within 24 h.

Similar, but more pronounced spectral changes also occurred in the CoTSPc reaction with basic thiolates (Fig. 3); the quantitative differences between Figs. 2A and 3 are discussed in the next two sections. The observed spectral changes indicate the formation of two different forms of phthalocyanine complexes, within two distinctly different ranges of thiolate concentrations; presumably, 1:1 and 2:1 thiolate-CoTSPc. Based on their broadened low-intensity absorption bands, high ionic strength of the solution (0.6 M) and aggregation of the other forms of CoTSPc, these complexes appear to be present in aqueous solutions as dimers or oligomers.

Additional evidence for this hypothesis was obtained from binding studies. Experimental data for all of the thiolates tested were found to be linear, within a wide range of thiolate concentrations, in double-reciprocal plots (Fig. 2B, right straight line), indicating 1:1 CoTSPc–thiolate binding at low thiolate concentrations (2:1 binding is covered in the next section). The values of 1:1 CoTSPc–thiolate binding constants, K_{RS1}, corresponding to the equilibrium constant in Reaction 2, were calculated from the corresponding double-reciprocal plots as x-intercepts outlined in Section 2 under Section 2.2.2 (Table 1A, column 3).

Based on the values of the binding constants, it was assessed that in our previous study their numerical values were underestimated because true equilibrium was not reached [35]. The reason for this miscalculation was the unusually long lag periods and slow rate of residual cobalt reduction, characteristic of low-basicity thiolates (Fig. 1, Steps 1, 3 and 6) which will be discussed under Section 3.2. We have corrected this error and obtained the true equilibrium constant values in this study, by increasing the reaction time to 6–7 days (Table 1A, column 3).

The binding constant values ($K_{RS\text{-}1}$) are similar in magnitude to those obtained in a non-aqueous solvent, *N*,*N*-dimethyl formamide (DMF) [34]. In DMF, CoTSPc is a monomer, whereas under the conditions used in the present study (ionic strength of 0.6 M) it is oligomeric. Therefore, CoTSPc aggregation in aqueous solutions does not appear to be a significant factor affecting the binding of the *first* thiolate equivalent.

The experimental binding constants do not correspond to any particular step in Fig. 1 because the product is not a single chemical, but rather an equilibrium mixture of the CoTSPc–thiolate complexes containing reduced and non-reduced cobalt, $K_{RS\text{-}1} = K_{12}K_{13\,red}$. Nevertheless, $K_{13\,red}$ can be obtained separately based on the fraction of reduced cobalt (see Section 2). The values of $K_{13\,red}$ are listed in Table 1B, column 5. (All the constants listed in Table 1B are derived from the data provided in Table 1A.) Based on these values, cobalt reduction is more pronounced for thiolates of

Table 1A
Experimental equilibrium constants for various thiolates

Substrate	pK_a	$K_{RS\text{-}1}$ (M^{-1})	$K_{RS\text{-}2}$ (M^{-1})	Fraction of Co^{I}TSPc (reduced) form	
				1:1 Complexes	2:1 Complexes
EtOCSSK	2.5 ± 0.1[36]	$(2.6 \pm 0.3) \times 10^2$[36]	$(5.0 \pm 0.6) \times 10^1$	$(2.8 \pm 0.2) \times 10^{-1}$[36]	$(4.6 \pm 0.4) \times 10^{-1}$
$(EtO)_2PSSNa$	2.7 ± 0.2	$(1.4 \pm 0.2) \times 10^2$	$(1.0 \pm 0.1) \times 10^1$	$(2.7 \pm 0.2) \times 10^{-1}$	$(4.6 \pm 0.4) \times 10^{-1}$
K_2CS_3	2.7 ± 0.2	$(2.3 \pm 0.2) \times 10^2$	$(1.0 \pm 0.1) \times 10^2$	$(2.7 \pm 0.2) \times 10^{-1}$	$(4.6 \pm 0.4) \times 10^{-1}$
$Et_2NCSSNa$	3.3 ± 0.2	$(1.7 \pm 0.1) \times 10^3$	N/A*	$(2.8 \pm 0.2) \times 10^{-1}$	N/A*
CH_3COSK	3.6 ± 0.2	$(1.9 \pm 0.2) \times 10^4$	$(3.6 \pm 0.4) \times 10^2$	$(3.6 \pm 0.3) \times 10^{-1}$	$(5.0 \pm 0.4) \times 10^{-1}$
Na_3PO_3S	4.5 ± 0.3 (1.6 ± 0.2)	$(3.8 \pm 0.3) \times 10^3$	$(1.1 \pm 0.2) \times 10^2$	$(3.3 \pm 0.2) \times 10^{-1}$	$(5.1 \pm 0.4) \times 10^{-1}$
Cysteine	8.2 [24]	$(1.7 \pm 0.2) \times 10^4$	$(6.0 \pm 0.5) \times 10^2$	$(5.0 \pm 0.5) \times 10^{-1}$	$(7.1 \pm 0.6) \times 10^{-1}$
HOC_2H_4SNa	9.2 [10]	$(2.8 \pm 0.2) \times 10^4$	$(1.5 \pm 0.1) \times 10^3$	$(6.9 \pm 0.6) \times 10^{-1}$	$(8.9 \pm 0.8) \times 10^{-1}$

Experiments were conducted under anaerobic conditions in 0.15 M borate buffer, pH 10.5, ionic strength 0.60 M. The concentration of CoTSPc was 1.0×10^{-5} M.
* N/A—not applicable because CoTSPc does not form a dithiolate complex with this substrate.

Table 1B
Equilibrium constants of Fig. 1 calculated for various thiolates from experimentally obtained parameters listed in Table 1A

Substrate	pK_a	K_{12} (M^{-1}) 1:1 complexes	K_{25} (M^{-1}) 2:1 complexes	$K_{13\ red}$ 1:1 complexes	$K_{26\ red}$ 2:1 complexes
EtOCSSK	2.5 ± 0.1 [36]	$(7 \pm 1) \times 10^2$	$(5.9 \pm 0.9) \times 10^1$	0.39 ± 0.04	0.85 ± 0.08
$(EtO)_2PSSNa$	2.7 ± 0.2	$(3.8 \pm 0.7) \times 10^2$	$(1.2 \pm 0.2) \times 10^1$	0.37 ± 0.04	0.85 ± 0.08
K_2CS_3	2.7 ± 0.2	$(6.2 \pm 0.9) \times 10^2$	$(1.2 \pm 0.2) \times 10^2$	0.37 ± 0.04	0.85 ± 0.08
$Et_2NCSSNa$	3.3 ± 0.2	$(4.4 \pm 0.5) \times 10^3$	N/A*	0.39 ± 0.04	N/A*
CH_3COSK	3.6 ± 0.2	$(3.4 \pm 0.5) \times 10^4$	$(3.6 \pm 0.5) \times 10^2$	0.56 ± 0.06	1.0 ± 0.1
Na_3PO_3S	4.5 ± 0.3 (1.6 ± 0.2)	$(8 \pm 1) \times 10^3$	$(1.0 \pm 0.2) \times 10^2$	0.49 ± 0.05	1.1 ± 0.1
Cysteine	8.2 [24]	$(1.7 \pm 0.3) \times 10^4$	$(2.5 \pm 0.3) \times 10^2$	1.0 ± 0.1	2.4 ± 0.2
HOC_2H_4SNa	9.2 [10]	$(1.4 \pm 0.2) \times 10^4$	$(1.7 \pm 0.2) \times 10^2$	2.0 ± 0.2	9 ± 1

* N/A—not applicable because CoTSPc does not form a dithiolate complex with this substrate.

higher basicity, as expected (Tables 1A and 1B, columns 5, Fig. 4).

Using the numerical values of $K_{RS\text{-}1}$ and $K_{13\ red}$, we also estimated the corresponding K_{12} values (Table 1B, column 3). As anticipated, based on the increase of K_{12} with the thiolate basicity (Fig. 5), thiolate binding by Co^{II}TSPc in aqueous solutions appears to be electron-donor in nature (Table 1B, column 3, Fig. 5).

3.1.2. *Second thiolate equivalent: evidence of binding*

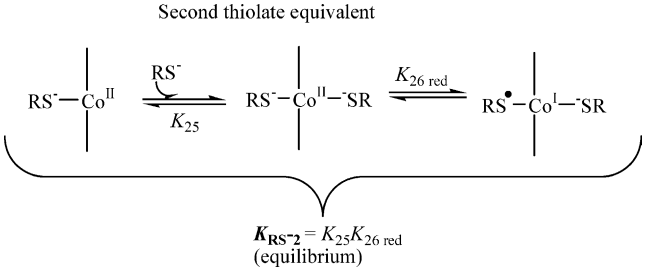

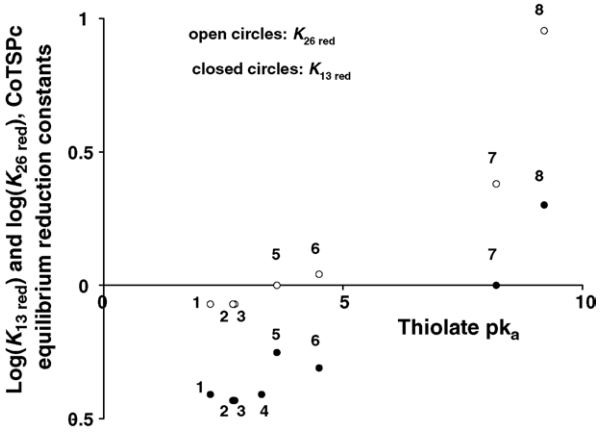

Fig. 4. Double-logarithmic plot of equilibrium constants $K_{13\ red}$ and $K_{26\ red}$, corresponding to Co^{II}–Co^{I} reduction in 1:1 and 2:1 thiolate–CoTSPc complexes, respectively, vs. the K_a of the conjugate acid. The numerical values are listed in Table 1B. Roman numerals correspond to substrates (1—EtOCSSK; 2—K_2CS_3; 3—$(EtO)_2PSSNa$; 4—$Et_2NCSSNa$; 5—CH_3COSK; 6—Na_3PO_3S; 7—Cys; 8—HOC_2H_4SNa).

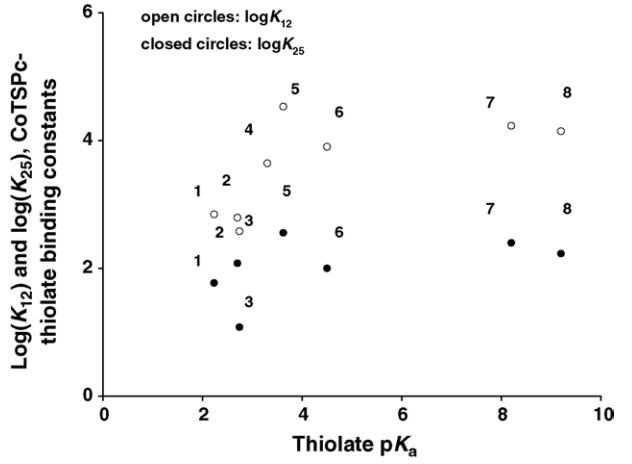

Fig. 5. Double-logarithmic plot of CoTSPc–thiolate binding constants K_{12} and K_{25} vs. the K_a of the conjugate acid. The numerical values are listed in Table 1B. Roman numerals correspond to substrates (1—EtOCSSK; 2—K_2CS_3; 3—$(EtO)_2PSSNa$; 4—$Et_2NCSSNa$; 5—CH_3COSK; 6—Na_3PO_3S; 7—Cys; 8—HOC_2H_4SNa).

Table 2A
Experimental equilibrium constants for four different alkyl xanthogenates

Substrate	pK_a [36]	$K_{RS\text{-}1}$ (M^{-1}) [36]	$K_{RS\text{-}2}$ (M^{-1})	Fraction of Co^{I}TSPc (reduced) form	
				1:1 Complex [36]	2:1 Complex
Ethyl xanthogenate	2.5 ± 0.1	$(2.6 \pm 0.3) \times 10^2$	$(5.0 \pm 0.6) \times 10^1$	$(2.8 \pm 0.2) \times 10^{-1}$	$(4.6 \pm 0.4) \times 10^{-1}$
n-Butyl xanthogenate	2.5 ± 0.1	$(7.4 \pm 0.3) \times 10^2$	$(6.0 \pm 0.6) \times 10^1$	$(3.0 \pm 0.2) \times 10^{-1}$	$(5.5 \pm 0.5) \times 10^{-1}$
n-Hexyl xanthogenate	2.5 ± 0.1	$(1.3 \pm 0.1) \times 10^3$	$(1.5 \pm 0.2) \times 10^2$	$(3.3 \pm 0.3) \times 10^{-1}$	$(6.5 \pm 0.6) \times 10^{-1}$
n-Octyl xanthogenate	2.5 ± 0.1	$(2.9 \pm 0.2) \times 10^3$	$(2.0 \pm 0.2) \times 10^2$	$(3.5 \pm 0.4) \times 10^{-1}$	$(7.7 \pm 0.7) \times 10^{-1}$

Experiments were conducted under anaerobic conditions in 0.15 M borate buffer, pH 10.5, ionic strength 0.60 M. The concentration of CoTSPc was 1.0×10^{-5} M.

Table 2B
Equilibrium constants of Fig. 1 calculated for four different alkyl xanthogenates from experimentally obtained parameters listed in Table 2A

Substrate 1	pK_a [36]	K_{12} (M^{-1}) 1:1 complex	K_{25} (M^{-1}) 2:1 complex	$K_{13\,red}$ 1:1 complex	$K_{26\,red}$ 2:1 complex
Ethyl xanthogenate	2.5 ± 0.1	$(7 \pm 1) \times 10^2$	$(5.9 \pm 0.9) \times 10^1$	0.39 ± 0.04	0.85 ± 0.08
n-Butyl xanthogenate	2.5 ± 0.1	$(1.7 \pm 0.2) \times 10^3$	$(5.0 \pm 0.6) \times 10^1$	0.43 ± 0.04	1.2 ± 0.1
n-Hexyl xanthogenate	2.5 ± 0.1	$(2.7 \pm 0.3) \times 10^3$	$(8 \pm 1) \times 10^1$	0.49 ± 0.05	1.9 ± 0.2
n-Octyl xanthogenate	2.5 ± 0.1	$(5.4 \pm 0.6) \times 10^3$	$(6.7 \pm 0.9) \times 10^1$	0.54 ± 0.05	3.0 ± 0.3

As shown in Fig. 2A, the CoTSPc spectral features change upon increase in ethyl xanthogenate concentration, from 1×10^{-4} to 1×10^{-2} M (fifth curve from the top). Then, they remain virtually unchanged upon further increase in substrate concentration up to $(2–3) \times 10^{-2}$ M (these concentration ranges varied for different ligands), indicating the metal's saturation by the ligand (sixth curve from the top). However, when the thiolate concentration is increased beyond this saturation range, a new change in the equilibrium CoTSPc–thiolate absorption spectra is observed (Fig. 2A). Of note is a shift in the isosbestic point from 534 to 570 nm, which no longer includes the original Co^{II}TSPc spectrum. Similar features were observed for basic thiolates (Fig. 3). Such spectral changes are consistent with the formation of two successive species from the reactant, i.e., sequential binding of two thiolate molecules (Fig. 1). The formation of two intermediates was also confirmed by an SVD analysis.

The corresponding double-reciprocal plot extended to these high thiolate concentrations becomes a combination of two straight lines, which is consistent with the proposed hypothesis (Fig. 2B). The binding constants for the second thiolate equivalent were calculated from the straight lines (with a steeper slope) as *x*-intercepts; they are listed in Table 1A, column 4.

3.1.3. Second thiolate molecule binding: effects of ligand's basicity

As for the binding of the first thiolate equivalent, we were able to separate the contributions of ligand binding to Co^{II}TSPc and the ensuing cobalt reduction; $K_{RS\text{-}2} = K_{25}K_{26\,red}$. The corresponding equilibrium constants from Fig. 1 are listed in Table 1B, column 4. The values of K_{25} (second thiolate equivalent's binding constant to Co^{II}TSPc) are significantly smaller in magnitude than those for the first thiolate molecule, K_{12}, as expected for binding of electron-donor ligands. For a similar reason (prior binding of an electron-donor ligand), K_{25}, unlike K_{12}, is nearly constant within a wider range of thiolate's pK_a, 2–9.5 (Fig. 5).

The electron-donor character of the second thiolate binding, however, shows up in the larger values of $K_{26\,red}$ as compared to $K_{13\,red}$ (Table 1B, columns 5, 6) and in the increase of $K_{26\,red}$ along with thiolate basicity (Fig. 4). These considerations are supported by direct spectral observations. For basic thiolates (pK_a > 4), the absorption peak of the thiolate–CoTSPc complex gradually shifts from 650 to 680 nm (Fig. 3), whereas for low-basicity thiolates this shift is less pronounced (Fig. 2A). For both types of thiolates, the absorbance at 450 nm corresponding to Co^{II}–Co^{I} reduction increases concomitantly. For basic thiolates, the final spectrum at saturating ligand concentrations [$(3–5) \times 10^{-1}$ M] becomes more consistent with that of the pure Co^{I}TSPc (Fig. 3); whereas for low-basicity thiolates the cobalt reduction is far from completion at any ligand concentration (Fig. 2A).

3.1.4. Hydrophobic effects in thiolate–CoTSPc binding and reduction

Hydrophobic effects in CoTSPc–thiolate binding were investigated using alkyl xanthogenates (organic compounds with the common formula $ROC(S)S^-M^+$; M = Na, K) with varied alkyl chain length, as was done previously for the first ligand's equivalent [36]. The experimentally measured binding constants are listed in Table 2A, whereas the derived equilibrium constants of the reaction scheme in Fig. 1 are listed in Table 2B.

The separation of binding and reduction equilibrium constants achieved in this study leads to the following observations. For the first thiolate molecule, a sizable increase in binding constant values from ethyl through octyl xanthogenate ($K_{RS\text{-}1}$, Table 2A, column 3) is not accounted for by an increase in the degree of cobalt reduction (Table 2A, column 5). It can be seen that the binding constant of the non-reduced Co^{II}TSPc, K_{12}, also increases in this series

(Table 2B, column 3), thus indicating a hydrophobic effect. Conversely, for the second thiolate, a small increase in the experimental binding constant values, $K_{RS\text{-}2}$, while increasing the ligand's hydrophobicity from ethyl through octyl xanthogenate (Table 2A, column 4), is accounted for by an increase in the extent of cobalt reduction (Table 2A, column 6). The corresponding Co^{II}TSPc binding constant, K_{25}, is nearly constant for all four alkyl xanthogenates (Table 2B, column 4).

Apparently, unlike the binding of the first ligand, there is no *true* hydrophobic effect in the attachment of the second thiolate molecule to CoTSPc. Larger alkyl groups create a less polar microenvironment, thus destabilizing any charge separation between the ligand and metal to promote the cobalt reduction, which in turn leads to the stronger binding. Indeed, spectral changes observed upon the CoTSPc reaction with hydrophobic hexyl- and octyl-xanthogenates (not shown) are similar to those depicted in Fig. 3, i.e., a more pronounced cobalt reduction is observed than that with less hydrophobic ethyl- and *n*-butyl xanthogenates (Fig. 2A).

3.1.5. Second thiolate binding: possible steric effects and connection to CoTSPc aggregation

We did not observe any second equivalent's binding for one of the substrates, $Et_2NCSSNa$, even upon increasing its concentration up to 0.5 M. This occurrence may be due to steric factors because the other bulky thiolate, $(EtO)_2PSSNa$, exhibits an order of magnitude smaller value of $K_{RS\text{-}2}$ (and K_{25}) as compared to K_2CS_3, a non-bulky substrate of the same basicity (Tables 1A and 1B, column 4). It is of note that the difference in 1:1 thiolate–CoTSPc binding constants for these two substrates is much less pronounced (Tables 1A and 1B, column 3). This observation indicates a significant physical constraint for the *second* rather than first thiolate molecule binding. Such a thermodynamic steric effect would be impossible for monomeric CoTSPc–thiolate complexes because, given ample time, there is enough room for both thiolates on two different sides of the equatorial phthalocyanine ligand. The CoTSPc dimeric (oligomeric) nature may be a reason for thermodynamic steric effects in binding constants.

Simple geometric considerations indicate that when CoTSPc–dithiolate complexes exist as dimers or oligomeric stacks, interactions are inevitable between two ligands that have to be located on the same side of the phthalocyanine plane (Fig. 6). Therefore, if the second thiolate is too bulky, this complex does not form at all because the alternative would be breaking up the stack.

Two possible molecular arrangements in dithiolate complexes are shown in Fig. 6A and B. The arrangement shown in Fig. 6A assumes thiolate "sandwiching" between the phthalocyanine planes; this is more consistent with the observed steric hindrance. However, this structure must have a rather tight "packing" because the presence of any molecules between the phthalocyanine planes would increase the distance between them, thus greatly reducing the likelihood of

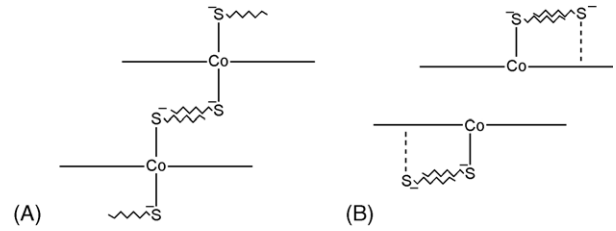

Fig. 6. Possible arrangement of 2:1 thiolate–CoTSPc complexes in dimers (oligomers).

the exciton coupling that results in the appearance of broadened lines in the UV–vis spectra. On the other hand, the more plausible structure shown in Fig. 6B can exist only as a dimer; also, a non-coordinating binding of one of the two thiolates is assumed. The possibility of an outer-sphere thiolate binding by CoTSPc is discussed is the next section on kinetics.

Our earlier studies indicated that aromatic thiolates that break the phthalocyanine oligomers to yield monomeric 1:1 thiolate–Co^{II}TSPc complexes do not form 2:1 complexes (checked up to the thiolate concentration of 0.5 M [35]). Also, the formation of 2:1 thiolate–CoTSPc complexes in DMF and other aprotic solvents where CoTSPc exists as a monomer was not observed [34]. Yet, upon increasing the thiolate concentration in DMF up to the level where the binding of the second thiolate molecule takes place in aqueous solutions [$(1\text{–}3)\times10^{-2}$ M], partial CoTSPc precipitation was observed, which becomes more pronounced at higher thiolate concentrations. Apparently, binding of the second thiolate equivalent to CoTSPc results in the formation of an oligomeric species that is insoluble in DMF.

It can therefore be concluded that oligomeric stacks tend to stabilize CoTSPc–*di*thiolate complexes. Evidently, the affinity of two CoTSPc equatorial phthalocyanine ligands to each other in stacked 1:1 thiolate complexes is stronger than that to the additional axial ligands, i.e., thiolate molecules. Comparison of the magnitude of stability constants for CoTSPc–to–CoTSPc (10^5 M^{-1} at 58 °C in aqueous solutions [22]) and (RS^-)CoTSPc–to–RS^- 2:1 complexes (10^2 M^{-1}, Table 1B, column 4) confirms this suggestion.

3.2. Kinetic studies

3.2.1. Kinetic curves at low thiolate concentrations: lag periods (Step 1 in Fig. 1)

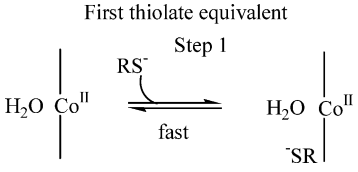

For all of the low-basicity thiolates used in this study ($pK_a < 5$), Reaction 2 kinetic curves include three steps (Fig. 7A). The rates of all three steps are first-order with respect to CoTSPc in a 1×10^{-6} to 5×10^{-4} M concentration range (not shown). Below, each step is analyzed separately in

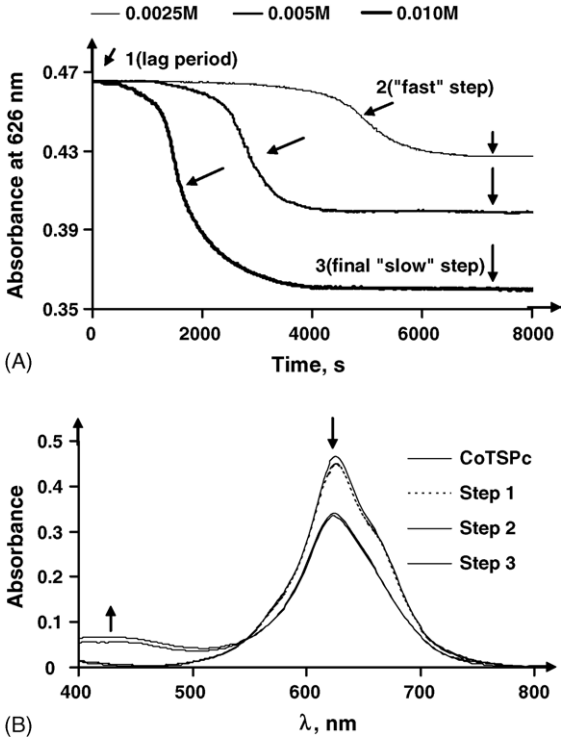

Fig. 7. (A) CoTSPc–*n*-butyl xanthogenate complexation kinetic curves observed in aqueous solutions for the attachment of the first thiolate molecule. The 626-nm CoTSPc absorbance was monitored under anaerobic conditions. Co^{II}TSPc concentration was 1.0×10^{-5} M (borate buffer [0.15 M], pH 10.5, ionic strength 0.60 M). *n*-Butyl xanthogenate concentration is shown in the legend. Step 1: lag period; Step 2: "fast" step; Step 3: final "slow" step. (B) UV–vis spectra of 1.0×10^{-5} M CoTSPc in the presence of 1.0×10^{-2} M *n*-butyl xanthogenate recorded after the completion of the corresponding kinetic steps (part A) under anaerobic conditions. Borate buffer (0.15 M), pH 10.5, ionic strength 0.60 M.

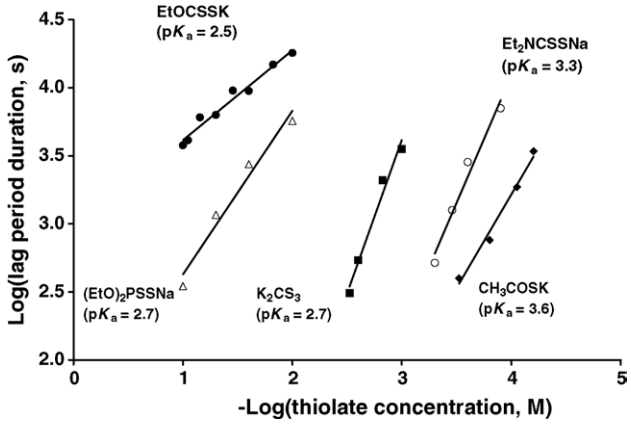

Fig. 8. Double-logarithmic plot: duration of the lag period vs. thiolate concentration. Concentration of CoTSPc was 1.0×10^{-5} M (borate buffer [0.15 M], pH 10.5, ionic strength 0.60 M, under anaerobic conditions).

more detail, separating the impact of CoTSPc reaction with the second thiolate equivalent from other factors.

The first step in kinetic curves is a lag period (Fig. 7A). During this lag period, there is no significant change in the entire Co^{II}TSPc spectrum; only a small decrease in the absorbance at 626 nm occurs (Fig. 7B, Step 1). No concomitant increase in the intensity of the 450-nm band was observed; thus, no $Co^{II} \rightarrow Co^{I}$ reduction occurs during this step. Apparently, as previously suggested [36], the thiolate reacts with Co^{II}TSPc by forming an outer-sphere complex (spectrophotometrically indistinguishable from the initial Co^{II}TSPc), in which sulfur is not directly attached to Co^{II} (Fig. 1). This cannot be an inner-sphere coordination thiolate complex of CoTSPc because those are characterized by strong absorption in a 660–690 nm range [34].

3.2.2. *Effect of the thiolate basicity on the duration of the lag period*

The duration of the lag period depends on the Co^{II}TSPc and substrate concentrations. It decreases with an increase in the concentration of either Co^{II}TSPc (1.0×10^{-6} to 1.0×10^{-4} M, not shown) or the thiolate (Fig. 8). This observation corroborates with Fig. 1 because an increase in concentrations accelerates both of the competing reactions. This, in turn, leads to preferred formation of a more stable axial thiolate–cobalt coordination complex, thus exerting thermodynamic control.

The lag period's duration also depends on the thiolate basicity (Fig. 8). It can be seen from Table 3 that a similar lag period duration was observed at significantly lower concentrations for more basic thiolates. The dependence of the lag period on thiolate basicity can be explained by an increase in binding constants, $K_{RS\text{-}1}$ or K_{12}, i.e., also by thermodynamic control (Tables 1A and 1B, columns 3). A similar effect is caused by increasing the ligand's hydrophobicity, which is also consistent with thermodynamic control [36].

Table 3
Thiolate concentrations at which the lag period duration was similar for different substrates

Substrate	pK_a	Concentration (M)	Lag period duration (s)
EtOCSSK	2.5 ± 0.1 [31]	1.0×10^{-1}	$(3.5 \pm 0.5) \times 10^{3}$ [36]
K_2CS_3	2.7 ± 0.2	1.0×10^{-3}	$(3.5 \pm 0.4) \times 10^{3}$
$(EtO)_2PSSNa$	2.7 ± 0.2	2.5×10^{-2}	$(2.8 \pm 0.3) \times 10^{3}$
$Et_2NCSSNa$	3.3 ± 0.2	2.5×10^{-4}	$(2.9 \pm 0.3) \times 10^{3}$
CH_3COSK	3.6 ± 0.2	1.0×10^{-4}	$(3.3 \pm 0.4) \times 10^{3}$
Na_3PO_3S	4.5 ± 0.3 (1.6 ± 0.2)	1.0×10^{-2}	$(3.0 \pm 0.3) \times 10^{3}$

Experiments were conducted under anaerobic conditions in 0.15 M borate buffer, pH 10.5, ionic strength 0.60 M. The concentration of CoTSPc was 1.0×10^{-5} M. The end of the lag period was defined as the time when the CoTSPc–thiolate complexation rate increased by at least 80% compared to the rate during the lag period.

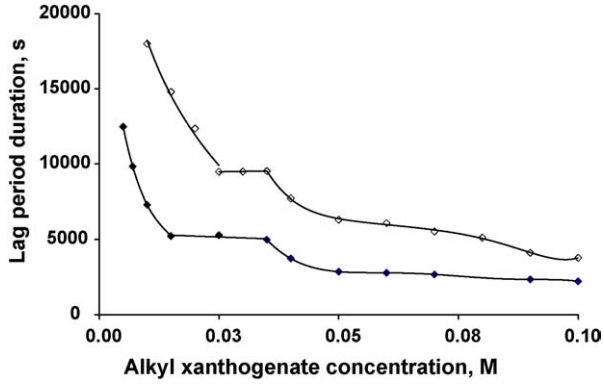

Fig. 9. Duration of the lag period for ethyl- and *n*-butyl xanthogenates at varied thiolate concentrations. Open rhombs: ethyl xanthogenate; close rhombs: butyl xanthogenate. Concentration of CoTSPc was 1.0×10^{-5} M (borate buffer [0.15 M], pH 10.5, ionic strength 0.60 M, under anaerobic conditions).

Extrapolation of the linear trends shown in Fig. 8 to high-basicity thiolates, such as cysteine and HOC_2H_4SNa, results in very short, microsecond-scale, lag periods even for very low thiolate concentrations, e.g., in the range of 10^{-4} M. This explains why lag periods have not been observed for common Merox process substrates.

3.2.3. *Effect of binding of the second thiolate equivalent on the duration of lag periods (Step 4 in Fig. 1)*

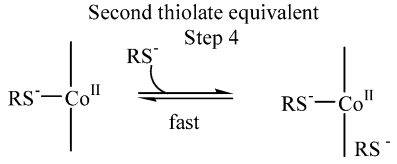

The plot of lag period's duration versus thiolate concentration is biphasic (Fig. 9, shown for ethyl- and *n*-butyl xanthogenates). Exceeding a certain threshold in the thiolate concentration results in a significant shortening of the lag period. This threshold lies within the concentration range where the binding of the second thiolate molecule starts taking place [$(1–3) \times 10^{-2}$ M]. Therefore, attachment of the second ligand greatly reduces the lifetime of the outer-sphere complex.

Kinetic curves at this intermediate range of thiolate concentrations are biphasic; a short but reproducible "lull," whose duration strongly depends on the thiolate concentration, occurs in the middle of the kinetic curve (Fig. 10A, Step 4). The UV–vis spectra recorded after Step 4 of the kinetic curves shown in Fig. 10A (Fig. 10B Step 4) are similar to those in Fig. 7B corresponding to the 1:1 thiolate–CoTSPc binding. However, the spectra taken after Steps 5 and 6, shown in Fig. 10A (Fig. 10B), are different from those obtained upon the 1:1 thiolate–CoTSPc binding (Fig. 7B). They are consistent, however, with binding of the *second* thiolate equivalent to CoTSPc at equilibrium (Fig. 2A, spectra at high thiolate concentrations). An SVD analysis (see Section 2.2) confirmed the formation of two intermediates with

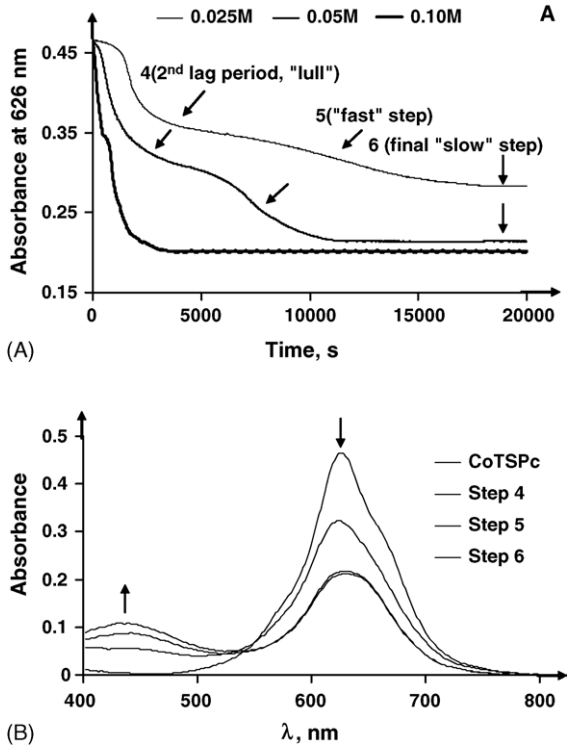

Fig. 10. (A) CoTSPc–*n*-butyl xanthogenate complexation kinetic curves observed in aqueous solutions for the attachment of the second thiolate molecule. The 626-nm CoTSPc absorbance was monitored under anaerobic conditions. Co^{II}TSPc concentration was 1.0×10^{-5} M (borate buffer [0.15 M], pH 10.5, ionic strength 0.60 M). *n*-Butyl xanthogenate concentration is shown in the legend. (B) UV–vis spectra of 1.0×10^{-5} M CoTSPc in the presence of 1.0×10^{-1} M *n*-butyl xanthogenate recorded after the completion of the corresponding kinetic steps (part A under anaerobic conditions. Borate buffer (0.15 M), pH 10.5, ionic strength 0.60 M.

the spectra similar to those obtained experimentally for 1:1 and 2:1 thiolate–CoTSPc complexes.

This observation provides a strong justification for the suggested reaction scheme (Fig. 1), showing that binding of two thiolate equivalents to CoTSPc is sequential and the coordination of each thiolate ligand to cobalt is preceded by the formation of a spectroscopically indistinguishable outer-sphere complex. Alternative kinetic schemes based on dissociative mechanisms or initiation of radical reactions considered earlier [36] may explain the presence of a lag period at the beginning of the reaction but not in the middle.

The presence of "lulls" in kinetic curves is more consistent with the hypothetical structure shown in Fig. 6A rather than Fig. 6B because the latter requires leaving the second thiolate outside of the cobalt coordination sphere. However, the proposed chemical structures can be verified only upon the isolation and characterization of the intermediates.

It is noteworthy that the "lulls" in kinetic curves are easily observed within a relatively broad concentration range (2.5×10^{-2}–1.0×10^{-1} M) only for *n*-butyl xanthogenate (Fig. 10A). For other substrates, this range is narrower and the "lulls" are shorter. Apparently, with the exception of $BuOCSS^-$, binding of the second thiolate occurs faster than

Table 4
Kinetic constants of Fig. 1 for various thiolates

Substrate	pK_a	$1/K_{M1}$ (M^{-1})	k_1 (min^{-1})	$1/K_{M2}$ (M^{-1})	k_2 (min^{-1})	k_{13} (min^{-1}) 1:1 complex	k_{26} (min^{-1}) 2:1 complex
EtOCSSK	2.5 ± 0.1 [36]	$(1.4 \pm 0.2) \times 10^2$ [36]	$(9.0 \pm 1.0) \times 10^{-3}$ [36]	$(5.5 \pm 0.6) \times 10^1$	$(2.8 \pm 0.3) \times 10^{-2}$	$(1.2 \pm 0.1) \times 10^{-5}$	$(2.2 \pm 0.2) \times 10^{-5}$
$(EtO)_2PSSNa$	2.7 ± 0.2	$(5.2 \pm 0.7) \times 10^1$	$(5.0 \pm 0.7) \times 10^{-2}$	6.1 ± 0.7	$(2.0 \pm 0.2) \times 10^{-1}$	$(1.2 \pm 0.1) \times 10^{-5}$	$(2.3 \pm 0.3) \times 10^{-5}$
K_2CS_3	2.7 ± 0.2	$(1.3 \pm 0.1) \times 10^2$	$(6.3 \pm 0.5) \times 10^{-2}$	$(4.7 \pm 0.6) \times 10^1$	$(2.2 \pm 0.2) \times 10^{-1}$	$(1.4 \pm 0.2) \times 10^{-5}$	$(2.5 \pm 0.3) \times 10^{-5}$
$Et_2NCSSNa$	3.3 ± 0.2	$(7.1 \pm 0.8) \times 10^2$	$(1.6 \pm 0.2) \times 10^{-1}$	N/A*	N/A*	$(1.6 \pm 0.2) \times 10^{-5}$	N/A*
CH_3COSK	3.6 ± 0.2	$(7.6 \pm 0.9) \times 10^3$	2.2 ± 0.3	$(2.1 \pm 0.3) \times 10^2$	9.8 ± 0.1	$(2.1 \pm 0.2) \times 10^{-5}$	$(3.8 \pm 0.4) \times 10^{-5}$
Na_3PO_3S	4.5 ± 0.3 (1.6 ± 0.2)	$(2.9 \pm 0.3) \times 10^3$	$(6.4 \pm 0.6) \times 10^{-1}$	$(1.0 \pm 0.2) \times 10^2$	4.9 ± 0.5	$(1.9 \pm 0.2) \times 10^{-5}$	$(3.1 \pm 0.3) \times 10^{-5}$
Cysteine	8.2 [24]	ND**	ND**	$(8.3 \pm 0.8) \times 10^1$ [24]	ND**	$(3.4 \pm 0.3) \times 10^{-5}$	$(5.2 \pm 0.5) \times 10^{-5}$
HOC_2H_4SNa	9.2 [10]	ND**	ND**	$(1.17 \pm 0.025) \times 10^2$ [10]	$(1.37 \pm 0.02) \times 10^4$ [10]	$(3.9 \pm 0.4) \times 10^{-5}$	$(8.1 \pm 0.9) \times 10^{-5}$

Experiments were conducted under anaerobic conditions in 0.15 M borate buffer, pH 10.5, ionic strength 0.60 M. The concentration of CoTSPc was 1.0×10^{-5} M.
* N/A—not applicable because CoTSPc does not form a dithiolate complex with this substrate.
** ND—not determined.

Table 5
Kinetic constants of Fig. 1 for four different alkyl xanthogenates

Substrate	pK_a [36]	$1/K_{M1}$ (M^{-1}) [36]	k_1 (min^{-1}) [36]	$1/K_{M2}$ (M^{-1})	k_2 (min^{-1})	k_{13} (min^{-1}) 1:1 complex	k_{26} (min^{-1}) 2:1 complex
Ethyl xanthogenate	2.5 ± 0.1	$(1.4 \pm 0.2) \times 10^2$	$(9.0 \pm 1.0) \times 10^{-3}$	$(5.5 \pm 0.6) \times 10^1$	$(2.8 \pm 0.3) \times 10^{-2}$	$(1.2 \pm 0.1) \times 10^{-5}$	$(2.2 \pm 0.2) \times 10^{-5}$
n-Butyl xanthogenate	2.5 ± 0.1	$(3.5 \pm 0.5) \times 10^2$	$(1.2 \pm 0.2) \times 10^{-2}$	$(5.7 \pm 0.8) \times 10^1$	$(8.1 \pm 0.8) \times 10^{-3}$	$(1.1 \pm 0.1) \times 10^{-5}$	$(2.2 \pm 0.2) \times 10^{-5}$
n-Hexyl xanthogenate	2.5 ± 0.1	$(1.0 \pm 0.1) \times 10^3$	$(1.9 \pm 0.3) \times 10^{-2}$	$(1.0 \pm 0.1) \times 10^2$	$(6.1 \pm 0.6) \times 10^{-2}$	$(1.2 \pm 0.1) \times 10^{-5}$	$(2.2 \pm 0.2) \times 10^{-5}$
n-Octyl xanthogenate	2.5 ± 0.1	$(2.0 \pm 0.3) \times 10^3$	$(2.4 \pm 0.4) \times 10^{-2}$	$(1.3 \pm 0.2) \times 10^2$	$(7.0 \pm 0.7) \times 10^{-2}$	$(1.2 \pm 0.1) \times 10^{-5}$	$(2.2 \pm 0.2) \times 10^{-5}$

Experiments were conducted under anaerobic conditions in 0.15 M borate buffer, pH 10.5, ionic strength 0.60 M. The concentration of CoTSPc was 1.0×10^{-5} M.

that of the first one, i.e., positive kinetic cooperativity exists. This suggestion was supported by the comparison of the corresponding kinetic constants, k_1 and k_2 (Tables 4 and 5, columns 4, 6) to be discussed in the following sections. The "lulls" were not observed for the substrates whose basicity is higher than that of Et_2NCSS^- because the reaction proceeds too fast.

3.2.4. *Kinetics of the thiolate–CoTSPc binding: calculation of kinetic constants (Steps 2 and 5 in Fig. 1)*

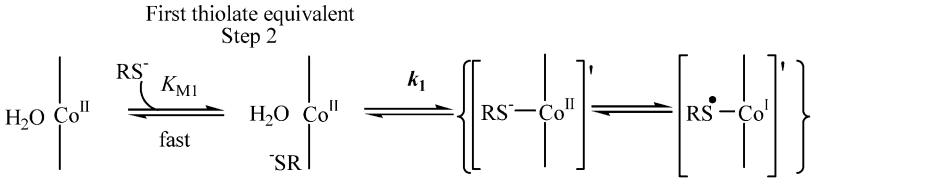

During the second step in kinetic curves, the absorbance at 626 nm drops relatively fast (Fig. 7A and B, Step 2). This is accompanied by an increase in absorbance at 450 nm. These spectral changes can be explained by the rearrangement of an outer-sphere complex into the corresponding inner-sphere coordination compound along with a partial Co^{II}–Co^{I} reduction (Reaction 2; Fig. 1, Step 2). It is noteworthy that the anions of thioacid salts can coordinate to Co in eta 1 or eta 2 fashion, which could not be distinguished.

Having plotted the rate of the second ("fast") step of the kinetic curve (Fig. 7A, Step 2) versus the thiolate concentration, a two-phase Michaelis-type plot was obtained for all thiolates used in this study (Fig. 11A), except for $Et_2NCSSNa$ which does not form a 2:1 complex. This further confirms the stepwise binding of two substrate equivalents to CoTSPc. Thus, the experimental results may be presented as two Michaelis–Menten kinetic equations:

$$\nu_1 = \frac{k_1[\text{CoTSPc}]_{\text{total}}[\text{RS}^-]}{K_{M1} + [\text{RS}^-]} \quad (3)$$

$$\nu_2 = \frac{k_2[\text{CoTSPc–RS}^-]_{\text{total}}[\text{RS}^-]}{K_{M2} + [\text{RS}^-]} \quad (4)$$

where ν_1 is the observed reaction rate of Co^{II}TSPc complexation with the first thiolate molecule; ν_2 is the reaction rate for the second thiolate equivalent; K_{M1} and K_{M2} are the corresponding Michaelis constants; and k_1 and k_2 are the turnover numbers for the first and second thiolate molecules, respectively.

For the reaction of CoTSPc with *n*-butyl xanthogenate, when the kinetic curves for the reactions of the first and second thiolate equivalents were separated in time, the values of k_1 and k_2 were calculated directly, based on the rates of two separate processes (Fig. 10A). For other substrates, the data points for the second phase of the Michaelis plot (Fig. 11A, the upper part with higher rates corresponding to those in Fig. 11B in the left part of the plot) were obtained when the kinetic curves for sequential binding of two thiolate equivalents were not separated (see the previous section), thus yielding just one experimental value for the reaction rate, $\nu = \nu_1 + \nu_2$. Based on Eqs. (3) and (4), monomolecular kinetic constants, k_1 and k_2, are specific rates (per unit of

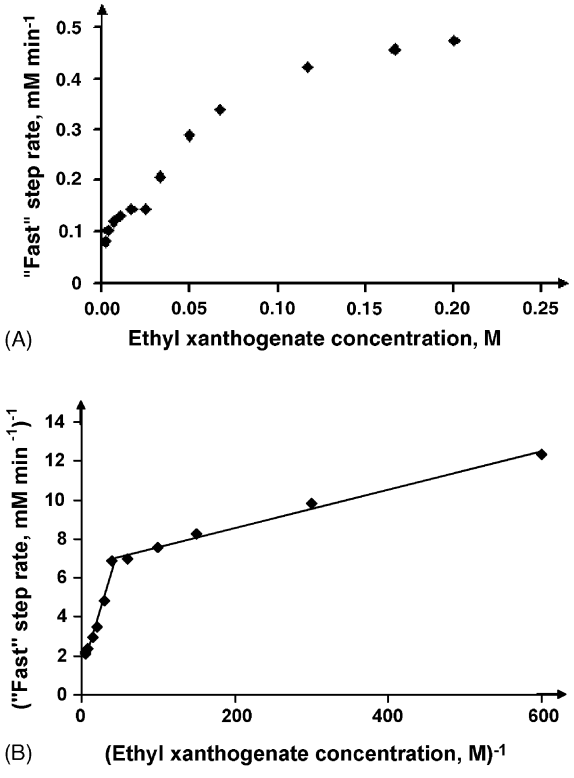

Fig. 11. (A) "Fast" step reaction rates (Steps 2 and 5 of Fig. 1 also see Figs. 7A and 10A) plotted at varied ethyl xanthogenate concentrations. Concentration of CoTSPc was 1.0×10^{-5} M (borate buffer [0.15 M], pH 10.5, ionic strength 0.60 M, under anaerobic conditions). (B) Double-reciprocal plot based on data from Fig. 11A.

CoTSPc concentration); therefore, these two constants are also additive when they are determined at saturating thiolate concentrations.

The values of the reciprocal Michaelis constants, $1/K_{M1}$, $1/K_{M2}$ and turnover numbers, k_1 and k_2 (experimental), were determined from the corresponding x- and y-intercepts of the double-reciprocal plot (Fig. 11B), respectively. The values of k_1 were calculated first, from the kinetics at low thiolate concentrations. Then, k_2 values were assessed using the additivity of kinetic constants, k_2 (experimental) = $k_1 + k_2$. Calculated kinetic parameters are listed in Tables 4 and 5 for ligands of varied basicity and hydrophobicity, respectively.

3.2.5. *Effect of ligand's basicity and hydrophobicity on kinetics of the thiolate–CoTSPc binding (Steps 2 and 5 in Fig. 1)*

As can be seen from Table 5, columns 4 and 6, kinetic constants k_1 and k_2 increase, although slightly, with thiolate hydrophobicity. However, they increase much more dramatically along with thiolate basicity (Table 4, columns 4, 6, Fig. 14). This observation indicates that the electron transfer from sulfur to cobalt appears to be the rate-limiting step. This is expected because the ultimate spectroscopically distinguishable products are Co^{I} species, whereas the reactant is Co^{II}TSPc; thus, the ligand–metal intramolecular electron transfer has to be the chemical essence of this process.

The reciprocal Michaelis constants are similar in magnitude to the corresponding binding constants (Tables 1B and 4, columns 3, 4 and 3, 5, respectively). They match even better the *pseudo*equilibrium constants $K'_{RS\text{-}1}$ and $K'_{RS\text{-}2}$ (see Table 7 below), i.e., not including the extremely slow final step (see next section), exhibiting similar trends as far as the influence of the ligand's basicity and hydrophobicity is concerned.

3.2.6. *The final slow kinetic step (Steps 3 and 6 in Fig. 1)*

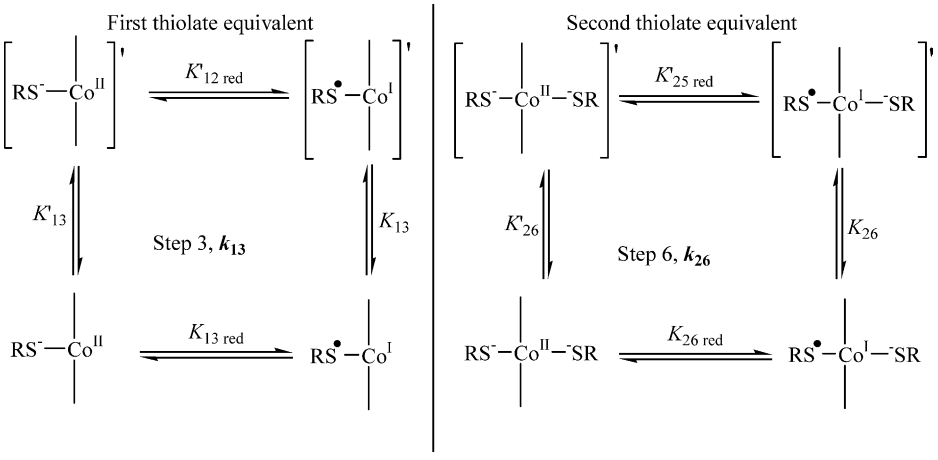

In the third, final, step in kinetic curves, a small but reproducible increase in 450 nm absorbance takes place accompanied by a small decrease of the other absorption maximum (Figs. 7A and B, Step 3). This indicates that only some residual Co^{II}–Co^{I} reduction occurs in the inner-sphere complex during this last step (Fig. 1, Step 3). UV–vis spectra taken after the completion of Steps 3 and 6 (Figs. 7B and 10B) do not show any changes in time. Thus, the final step is not an artifact related to thioacid hydrolysis or O_2 penetration into the glass cell, which, if happens, causes continued and significant increase in absorbance in the UV region (200–300 nm).

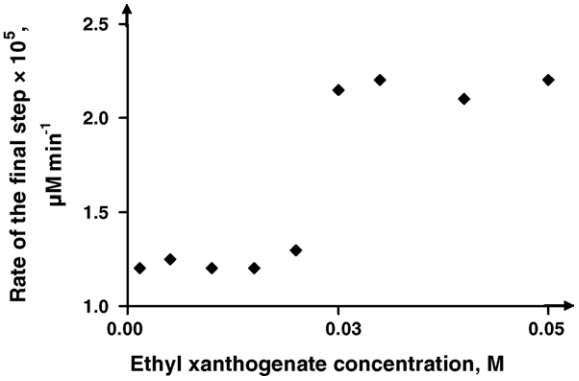

Fig. 12. Final step reaction rates plotted at varied ethyl xanthogenate concentrations. Concentration of CoTSPc was 1.0×10^{-5} M (borate buffer [0.15 M], pH 10.5, ionic strength 0.60 M, under anaerobic conditions).

The final step's rate is unusually slow, even if basic thiolates are used as substrates: it takes 4–7 days to reach equilibrium whereas the earlier steps are finished in a few hours (few seconds for basic thiolates, DL-cysteine and 2-mercaptoethanol).

The rate of the final step is zeroth-order with respect to thiolate within its concentration range of 1×10^{-3} to 2×10^{-2} M (Fig. 12). Zeroth kinetic order on thiolate is consistent with the suggested reaction scheme (Fig. 1) because at this stage all available CoTSPc is complexed with the thiolate, and only some intramolecular rearrangement occurs within the complex.

Upon increasing the thiolate concentration beyond $(2\text{–}3) \times 10^{-2}$ M, i.e., the concentration range of the 2:1 thiolate–CoTSPc binding (Fig. 10A, Step 6), the final step's

rate increases stepwise by a factor of 1.5–2 (Table 4, columns 7, 8). The rate does not change anymore upon further increase in thiolate concentration (zeroth-order in thiolate is maintained in the range of 3×10^{-3} to 2×10^{-1} M). This is consistent with a stepwise attachment of two thiolate equivalents to CoTSPc and allows for the separation of the two corresponding kinetic constants of Fig. 1, k_{13} and k_{26} (Table 4, columns 7 and 8).

The comparison of numerical values of kinetic constants shows that Step 3 (and 6) is not merely a continuation of Step 2 (and 5); k_{13} and k_{26} are several orders of magnitude smaller than k_1 and k_2, respectively. This also implies that the final step has to be placed in Fig. 1 *after* the rate-limiting step of the main reaction. Otherwise, reactions would continue at steady-state with the same kinetic constants as in the "fast" step, k_1 or k_2. Step 3 (and 6) is, essentially, a rather different reaction. The following information as to the effect of ligand's parameters on kinetics of Steps 2 (and 5) and 3 (and 6) confirms this suggestion.

The final step's rate is virtually the same for the four different alkyl xanthogenates (Table 5, columns 7 and 8). Therefore, unlike Step 2, it does not depend on thiolate hydrophobicity. The rate of the final step increases slightly with the increase in thiolate basicity (Table 4, columns 7 and 8). This is expected because Steps 3 and 6 are accompanied by some additional Co^{II} reduction. However, the comparison of the slopes of Brønsted equations for Steps 3 and 6 and preceding Steps 2 and 5, respectively, shows that the former are much less affected by the thiolate basicity than the latter (Table 6). Apparently, the chemical essence of the final step is not an electron transfer but some other factor. Adjustment in the degree of phthalocyanine aggregation and/or, perhaps, switching between the different arrangements shown in Fig. 6 may be just such a factor because this final step is not observed when the reaction is conducted in DMF [34]. However, no definitive conclusion about the nature of this reaction can be made based on the available information.

Table 6
Slopes of Brønsted correlations for the reaction kinetic constants (see Fig. 1 for Reaction 2)

Process	Kinetic constant	Brønsted slope
Step 2 of Fig. 1 (1:1 thiolate–CoTSPc binding)	k_1, Eq. (3)	0.9 ± 0.1
Step 5 of Fig. 1 (2:1 thiolate–CoTSPc binding)	k_2, Eq. (4)	0.8 ± 0.1
Merox process (Reaction 1)	k_{cat}, Eq. (5)	0.9 ± 0.1
Step 3 of Fig. 1 (1:1 thiolate–CoTSPc complex)	k_{13}	0.07 ± 0.02
Step 6 of Fig. 1 (2:1 thiolate–CoTSPc complex)	k_{26}	0.07 ± 0.02

The slow rate of this reaction allows for the calculation of pseudoequilibrium constants for the equilibria achieved upon the completion of Step 2 (and 5) (see Section 2), before Step 3 (and 6) takes off. They are listed in Tables 7A and 7B for the

Table 7A
Pseudoequilibrium constants for various substrates (1:1 complexes)

Substrate	pK_a	$K'_{RS\text{-}1}$ (M^{-1})	K'_{12} (M^{-1})	$K'_{12\,red}$	K'_{13}	K_{13}
EtOCSSK	2.5 ± 0.1 [36]	$(1.5 \pm 0.2) \times 10^2$	$(4.7 \pm 0.8) \times 10^2$	0.32 ± 0.03	1.4 ± 0.3	1.7 ± 0.2
n-Butyl xanthogenate	2.5 ± 0.1 [36]	$(4.2 \pm 0.6) \times 10^2$	$(1.2 \pm 0.2) \times 10^3$	0.35 ± 0.04	1.4 ± 0.3	1.7 ± 0.2
n-Hexyl xanthogenate	2.5 ± 0.1 [36]	$(7.2 \pm 0.9) \times 10^2$	$(1.8 \pm 0.3) \times 10^3$	0.39 ± 0.04	1.4 ± 0.3	1.8 ± 0.2
n-Octyl xanthogenate	2.5 ± 0.1 [36]	$(1.7 \pm 0.2) \times 10^3$	$(4.0 \pm 0.6) \times 10^3$	0.43 ± 0.04	1.4 ± 0.3	1.8 ± 0.2
$(EtO)_2PSSNa$	2.7 ± 0.2	$(1.1 \pm 0.2) \times 10^2$	$(3.7 \pm 0.8) \times 10^2$	0.30 ± 0.03	1.0 ± 0.3	1.2 ± 0.1
K_2CS_3	2.7 ± 0.2	$(1.8 \pm 0.2) \times 10^2$	$(6.0 \pm 0.9) \times 10^2$	0.30 ± 0.03	1.0 ± 0.2	1.2 ± 0.1
$Et_2NCSSNa$	3.3 ± 0.2	$(9 \pm 1) \times 10^2$	$(2.8 \pm 0.4) \times 10^3$	0.32 ± 0.03	1.6 ± 0.3	1.9 ± 0.2
CH_3COSK	3.6 ± 0.2	$(7.6 \pm 0.9) \times 10^3$	$(1.8 \pm 0.3) \times 10^4$	0.43 ± 0.04	1.9 ± 0.4	2.5 ± 0.3
Na_3PO_3S	4.5 ± 0.3 (1.6 ± 0.2)	$(3.2 \pm 0.3) \times 10^3$	$(8 \pm 1) \times 10^3$	0.39 ± 0.04	1.0 ± 0.2	1.3 ± 0.1
HOC_2H_4SNa	9.2 [10]	$(1.9 \pm 0.2) \times 10^4$	$(1.6 \pm 0.2) \times 10^4$	1.2 ± 0.1	0.9 ± 0.2	1.5 ± 0.2

Experiments were conducted under anaerobic conditions in 0.15 M borate buffer, pH 10.5, ionic strength 0.60 M. The concentration of CoTSPc was 1.0×10^{-5} M.

Table 7B
Pseudoequilibrium constants for various substrates (2:1 complexes)

Substrate	pK_a	$K'_{RS\text{-}2}$ (M^{-1})	K'_{25} (M^{-1})	$K'_{25\,red}$	K'_{26}	K_{26}
EtOCSSK	2.5 ± 0.1[36]	$(4.7 \pm 0.6) \times 10^1$	$(8 \pm 1) \times 10^1$	0.59 ± 0.06	0.7 ± 0.2	1.0 ± 0.1
n-Butyl xanthogenate	2.5 ± 0.1[36]	$(5.7 \pm 0.6) \times 10^1$	$(7 \pm 1) \times 10^1$	0.79 ± 0.08	0.7 ± 0.1	1.1 ± 0.1
n-Hexyl xanthogenate	2.5 ± 0.1[36]	$(1.2 \pm 0.2) \times 10^2$	$(1.1 \pm 0.2) \times 10^2$	1.1 ± 0.1	0.7 ± 0.2	1.2 ± 0.1
n-Octyl xanthogenate	2.5 ± 0.1[36]	$(1.6 \pm 0.2) \times 10^2$	$(1.1 \pm 0.2) \times 10^2$	1.4 ± 0.2	0.6 ± 0.1	1.3 ± 0.1
$(EtO)_2PSSNa$	2.7 ± 0.2	7 ± 1	$(1.2 \pm 0.2) \times 10^1$	0.59 ± 0.06	1.0 ± 0.2	1.4 ± 0.1
K_2CS_3	2.7 ± 0.2	$(6 \pm 1) \times 10^1$	$(1.0 \pm 0.2) \times 10^2$	0.59 ± 0.06	1.2 ± 0.3	1.7 ± 0.1
$Et_2NCSSNa$	3.3 ± 0.2	N/A*	N/A*	N/A*	N/A*	N/A*
CH_3COSK	3.6 ± 0.2	$(2.6 \pm 0.3) \times 10^2$	$(3.9 \pm 0.6) \times 10^2$	0.67 ± 0.07	0.9 ± 0.2	1.3 ± 0.1
Na_3PO_3S	4.5 ± 0.3 (1.6 ± 0.2)	$(9 \pm 1) \times 10^1$	$(1.3 \pm 0.2) \times 10^2$	0.69 ± 0.07	0.8 ± 0.2	1.3 ± 0.1
HOC_2H_4SNa	9.2 [10]	$(1.3 \pm 0.1) \times 10^3$	$(5.0 \pm 0.7) \times 10^2$	2.6 ± 0.3	0.3 ± 0.1	1.0 ± 0.1

Experiments were conducted under anaerobic conditions in 0.15 M borate buffer, pH 10.5, ionic strength 0.60 M. The concentration of CoTSPc was 1.0×10^{-5} M.
* N/A–not applicable because CoTSPc does not form a dithiolate complex with this substrate.

first and second thiolate equivalents, respectively. Since the spectral changes as a result of the final step are minimal, values of the binding constants obtained at pseudoequilibrium and at true equilibrium are similar in magnitude.

3.2.7. Comparison of Reaction 2 kinetics in DMF and aqueous solutions

In DMF, where CoTSPc is a monomer, no reaction with the second thiolate and no slow final step were observed [34]. This indicates that these reactions (Steps 3, 6) are characteristic only for aggregated thiolate–CoTSPc complexes. Yet, other basic kinetic features for the 1:1 reaction are similar [34]: the transient formation of both outer- and inner-sphere thiolate–Co^{II}TSPc complexes was observed, and the kinetic equation contains similar constants, k_1 ranged in $(2–7) \times 10^{-2}\,min^{-1}$ and K_{M1} ($1/K_{M1}$ ranged from 10^2 to $10^4\,M^{-1}$), as in aqueous media. However, unlike the reaction in aqueous media, the values of k_1 in DMF are virtually non-sensitive to thiolate basicity [34]. Therefore, in DMF the rate-limiting step appears to be just the "wiggling" of the axial thiolate ligand between the metal and equatorial phthalocyanine ligand while the ensuing electron transfer is faster. Comparison of numerical values of k_1 in both solvents confirms this suggestion: in DMF, for thiolates of low basicity (when electron transfer is expected to be slow) this parameter is at least one order of magnitude greater than in aqueous media, whereas for more basic thiolates they are comparable [34].

3.3. Merox process kinetics (Reaction 1)

3.3.1. Validation of the anaerobic reaction being a subset of the Merox process

A series of experiments on Merox process kinetics was conducted to connect the proposed mechanism of anaerobic Reaction 2 ("anaerobic" step in Scheme 1) with the overall mechanism of Reaction 1. The series of full kinetic curves were obtained using a wide range of thiolate concentrations, and then initial reaction rates were analyzed. Kinetic first-order dependence on the catalyst (CoTSPc) and oxygen [35] were observed regardless of thiolate type and concentration. Regarding the substrate concentrations, two different sets of kinetic features were observed. For substrates that contain alkyl groups (EtOCSSK, $(EtO)_2PSSK$, $Et_2NCSSNa$, CH_3COSK, cysteine [24] and also for HS^- and S^{2-} [26]), the Michaelis-type curves were obtained in a similar thiolate concentration range as for Reaction 2 (Fig. 13A) yielding the following kinetic equation:

$$v_{Merox} = \frac{k_{cat}[CoTSPc][RS^-][O_2]}{K_{M,\,Merox} + [RS^-]} \quad (5)$$

For inorganic substrates that contain sulfur, but cannot be viewed as alkyl thiolates (Na_3PO_3S, K_2CS_3), first-order kinetic dependence in thiolate was observed (Fig. 13B). Therefore, for true thiolates the mechanisms of Reactions 1 and 2 appear to be related, whereas for Na_3PO_3S and K_2CS_3 they are not.

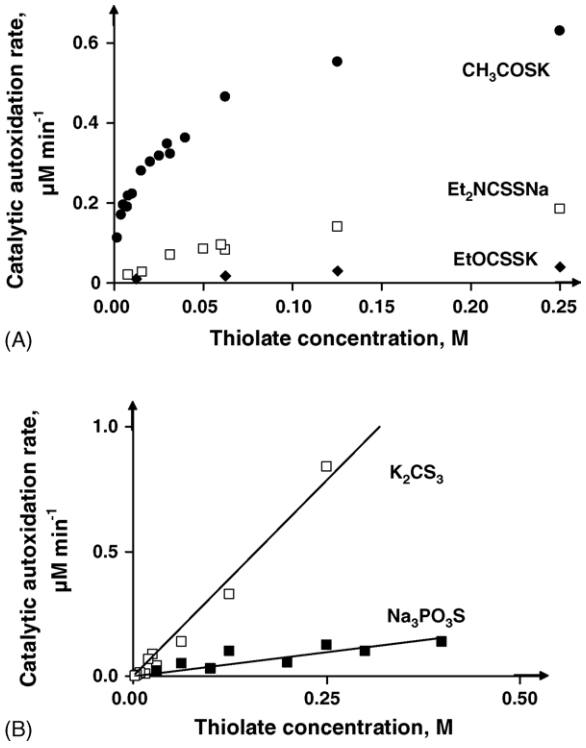

Fig. 13. (A) Autoxidation reaction rates (Merox process, Reaction 1) plotted for EtOCSSK, $Et_2NCSSNa$, and CH_3COSK at varied thiolate concentrations. Concentrations of CoTSPc and oxygen were 1.0×10^{-5} and $(2.0 \pm 0.1) \times 10^{-4}$ M, respectively (borate buffer [0.15 M], pH 10.5, ionic strength 0.60 M). (B) Autoxidation reaction rates (Merox process, Reaction 1) plotted for Na_3PO_3S and K_2CS_3 at varied substrate concentrations. Concentrations of CoTSPc and oxygen were 1.0×10^{-5} and $(2.0 \pm 0.1) \times 10^{-4}$ M, respectively (borate buffer [0.15 M], pH 10.5, ionic strength 0.60 M).

3.3.2. Participation of the second thiolate equivalent

Kinetic constants obtained upon linearization of the Michaelis curves as double-reciprocal plots are listed in Table 8. It can be seen that the values of Michaelis constants for Reaction 1, $K_{M,\,Merox}$ (Table 8, column 3) and the second K_{M2} of Reaction 2 (Table 4, column 5) are similar for all the thiolates tested, i.e., the anaerobic reaction (Reaction 2) appears to be a part of the aerobic one (as the "anaerobic" step of Reaction 1). The only exception was $Et_2NCSSNa$, for which 2:1 binding to CoTSPc was not observed in the anaerobic reaction.

It is of note that the Michaelis constants observed in the aerobic Merox process correspond to the binding constants of the *second* thiolate molecule in the anaerobic process (Tables 1A and 8, columns 4 and 3, respectively). This observation provides kinetic evidence of the involvement of *two* thiolate molecules in the mechanism of Reaction 1, and points out that thiolate–phthalocyanine binding is at fast equilibrium during the CoTSPc-catalyzed autoxidation (not including slow Steps 3 and 6 of the reaction scheme in Fig. 1).

Table 8
Merox process kinetic constants for various thiolates (Scheme 1)

Substrate	pK_a	$1/K_{M,\ Merox}$ (M^{-1})**	k_{cat} (min^{-1})
EtOCSSK	2.5 ± 0.1 [36]	$(4.8 \pm 0.5) \times 10^1$	$(6.2 \pm 0.7) \times 10^{-3}$
$(EtO)_2PSSNa$	2.7 ± 0.2	7.0 ± 0.7	$(5.6 \pm 0.6) \times 10^{-3}$
K_2CS_3	2.7 ± 0.2	N/A*	N/A*
$Et_2NCSSNa$	3.3 ± 0.2	$(1.1 \pm 0.1) \times 10^1$	$(2.4 \pm 0.2) \times 10^{-2}$
CH_3COSK	3.6 ± 0.2	$(2.0 \pm 0.2) \times 10^2$	$(3.7 \pm 0.3) \times 10^{-1}$
Na_3PO_3S	4.5 ± 0.3 (1.6 ± 0.2)	N/A*	N/A*
HS^-	7.8 [44]	1.7×10^2 [26]	1.6×10^2 [26]
Cysteine	8.2 [24]	$(7.8 \pm 1.8) \times 10^1$ [38]	6.3×10^2 [38]

Experiments were conducted in 0.15 M borate buffer, pH 10.5, ionic strength 0.60 M. The concentration of CoTSPc was 1.0×10^{-5} M.
* N/A—not applicable because the rate did not obey the Michaelis equation.
** Corresponds to K_{RS^-} in Scheme 1.

3.3.3. Rate-limiting step in the Merox process

Both the reciprocal Michaelis constants and first-order kinetic (catalytic) constants (k_{cat}) increase with the thiolate basicity, similar to the related parameters of Reaction 2 (Tables 4 and 8, columns 5, 6 and 3, 4, respectively). Furthermore, the catalytic constants exhibit good Brønsted correlation with a slope of 0.9 ± 0.1, which is statistically the same to the corresponding anaerobic constant slopes k_1 and k_2, 0.9 ± 0.1 and 0.8 ± 0.1, respectively (Fig. 14; Table 6). Thus, aerobic and anaerobic processes appear to be related and electron transfer appears to be a rate-limiting step in both.

Values of k_{cat} are 1–2 orders of magnitude smaller than those of the corresponding first-order constants of the CoTSPc–thiolate binding under anaerobic conditions, k_1 and k_2 (Table 4: columns 4, 6; Table 8: column 4; Fig. 14). This observation supports the suggestion that fast equilibrium for the thiolate–CoTSPc binding occurs during the Merox process. The Reaction 1 rate-limiting step appears to take place on or after oxygen binding by the phthalocyanine–thiolate complex. It can be noted that the slow final step of the anaerobic reaction (Steps 3 and 6 of Fig. 1) does not appear to have any effect on Reaction 1 because its rate is several orders of magnitude smaller than that of the Merox process.

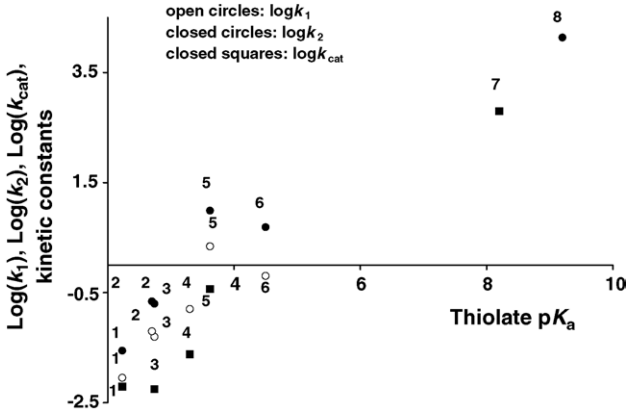

Fig. 14. Double-logarithmic plot of CoTSPc–thiolate kinetic constants k_1, k_2 and k_{cat} vs. the K_a of the conjugate acid. The numerical values are listed in Tables 4 and 8. Roman numerals correspond to substrates (1—EtOCSSK; 2—K_2CS_3; 3—$(EtO)_2PSSNa$; 4—$Et_2NCSSNa$; 5—CH_3COSK; 6—Na_3PO_3S; 7—Cys; 8—HOC_2H_4SNa).

Formation of the outer-sphere thiolate–phthalocyanine complexes postulated in this study explains how two thiolate molecules and O_2 can be simultaneously attached to one CoTSPc unit. No lag periods were observed in the Merox process even at low thiolate concentrations, thus indicating that the outer-sphere thiolate binding postulated immediately upon mixing the reagents appears to be sufficient for the catalytic reaction.

4. Conclusions

- Anaerobic reaction of CoTSPc with thiolates and anions of thioacids occurs as a stepwise attachment of two thiolate ligands. Each step is preceded by an outer-sphere thiolate binding resulting in the appearance of lag periods and "lulls" at the beginning and in the middle of kinetic curves, respectively. Binding of the second thiolate equivalent occurs at higher ligand concentrations and only if CoTSPc exists as a dimer (oligomer).
- The rate-limiting step of Reaction 2 appears to be the thiolate–Co^{II}TSPc electron transfer. The reaction is followed by another, separate process, apparently the rearrangement of stacked phthalocyanine aggregates, exhibited as a rather slow and small increase in the extent of cobalt reduction.
- Based on the comparison of kinetic constants, the aerobic Merox process appears to include the anaerobic process as a subset at fast equilibrium, requires the binding of two thiolate equivalents per one CoTSPc, and has a rate-limiting step of a similar nature.

Acknowledgements

The authors would like to thank Dr. T.P.M. Beelen, Eindhoven Technology University, The Netherlands, for providing CoTSPc, and Dr. A. Kubatova, University of North Dakota (UND) for help with MS experiments. This work was supported by UND Department of Chemistry. The authors

would also like to thank the UND Graduate School, Administration, and UND EPSCoR (NSF grant #EPS-0132289) for summer and travel support.

References

[1] B. Basu, S. Satapathy, A.K. Bhutnagar, Catal. Rev. 35 (1993) 571.
[2] T.A. Ananieva, G.F. Titova, V.F. Borodkin, Izv. Vyssh. Uchebn. Zaved. U.S.S.R., Ser. Khim; Khim. Tekhnol. 22 (1979) 37.
[3] G.F. Titova, T.A. Ananieva, T.E. Kuznetsova, Izv. Vyssh. Uchebn. Zaved. U.S.S.R., Ser. Khim; Khim. Tekhnol. 24 (1981) 445.
[4] T.A. Ananieva, G.F. Titova, V.F. Borodkin, Izv. Vyssh. Uchebn. Zaved. U.S.S.R., Ser. Khim; Khim. Tekhnol. 25 (1982) 706.
[5] V.E. Vigdergauz, A.K. Yatsimirskii, V.A. Chanturiya, E.I. Kozliak, V.V. Faydelj, A.S. Erokhin, M.V. Teplyakova, N.K. Gromova, USSR Patent 13,34,446 (1987).
[6] A.K. Yatsimirskii, E.I. Kozliak, A.S. Erokhin, V.E. Vigdergauz, I.V. Berezin, React. Kinet. Catal. Lett. 34 (1987) 439.
[7] J. Dolinsky, D.M. Wagnerova, J. Veprek-Siska, Collect. Czech. Chem. Commun. 41 (1976) 2326.
[8] W.M. Brouwer, P. Piet, A.L. German, J. Mol. Catal. 22 (1984) 297, and references therein.
[9] M.R. Hoffmann, A.P.K. Hong, Sci. Total Environ. 64 (1987) 99.
[10] P.-S.K. Leung, E.A. Betterton, M.R. Hoffmann, J. Phys. Chem. 93 (1989) 430.
[11] P.-S.K. Leung, M.R. Hoffmann, J. Phys. Chem. 93 (1989) 434.
[12] J. van Welzen, A.M. van Herk, A.L. German, Makromol. Chem. 189 (1988) 587.
[13] A.M. van Herk, A.H.J. Tullemans, J. van Welzen, A.L. German, J. Mol. Catal. 44 (1988) 269.
[14] E.T.W.M. Schipper, J.P.A. Heuts, R.P.M. Pinckaers, P. Piet, A.L. German, J. Polym. Sci. A: Polym. Chem. 33 (1995) 1841, and references therein.
[15] L.C. Gruen, J. Blagrove, Aus. J. Chem. 26 (1973) 319.
[16] E.W. Abel, J. Pratt, R. Whelan, J. Chem. Soc., Dalton Trans. (1976) 509.
[17] R.D. George, A.W. Snow, J.S. Shirk, W.R. Barger, J. Porphyrins Phthalocyanines 2 (1998) 1.
[18] A.B.P. Lever, M.R. Helmstead, C.C. Leznoff, W. Liu, M. Melnik, W.A. Nevin, P. Seymour, Pure Appl. Chem. 58 (1986) 1467.
[19] J.R. Darwent, J. Chem. Soc., Chem. Commun (1980) 805.
[20] J.R. Darwent, J. McCubbin, J. Porter, J. Chem. Soc., Faraday Trans. II (1982) 903.
[21] E.I. Kozliak, A.S. Erokhin, A.K. Yatsimirskii, J. Gen. Chem. (USSR) 12 (1988) 66.
[22] Z.A. Schelly, R.D. Farina, E.M. Eyring, J. Phys. Chem. 74 (1970) 617.
[23] E.I. Kozliak, A.S. Erokhin, A.K. Yatsimirskii, I.V. Berezin, Bull. Acad. Sci. USSR, Div. Chem. Sci. (1986) 741.
[24] E.I. Kozliak, A.S. Erokhin, A.K. Yatsimirskii, React. Kinet. Catal. Lett. 33 (1987) 113.
[25] A.K. Yatsimirskii, E.I. Kozlyak, A.S. Erokhin, Kinet. Catal. (USSR) 29 (1988) 305.
[26] H. Fisher, G. Schultz-Ekloff, D. Wöhrle, Chem. Eng. Technol. 20 (1997) 624.
[27] J. van Welzen, A.M. van Herk, H. Kramer, T.G.L. Thijssen, A.L. German, J. Mol. Catal. 59 (1990) 311.
[28] J. Zwart, H.C. van der Weide, N. Bröker, C. Rummens, G.C.A. Schuit, A.L. German, J. Mol. Catal. 3 (1977–1978) 151.
[29] N. d'Alessandro, L. Tonucci, L.K. Dragani, A. Morvillo, M. Bressan, J. Porphyrins Phthalocyanines 7 (2003) 484.
[30] J.A. De Bolfo, T.D. Smith, J.F. Boas, P.R. Hicks, J.R. Pilbrow, J. Chem. Soc., Dalton Trans. 109 (1977).
[31] A. Skorobogaty, T.D. Smith, J. Mol. Catal. 16 (1982) 131.
[32] T. Annesley, Clin. Chem. 49 (2003) 1041–1044.
[33] D.W. Dixon, A.F. Gill, B.R. Sook, J. Porphyrins Phthalocyanines 8 (2004) 1300.
[34] E.M. Tyapochkin, E.I. Kozliak, J. Porphyrins Phthalocyanines 5 (2001) 405.
[35] A. Navid, E.M. Tyapochkin, Ch.J. Archer, E.I. Kozliak, J. Porphyrins Phthalocyanines 3 (1999) 654.
[36] E.M. Tyapochkin, E.I. Kozliak, J. Mol. Catal. A: Chem. 203 (2003) 37.
[37] E.I. Kozliak, A. Navid, Prepr. ACS Div. Fuel Chem. 42 (1997) 56.
[38] E.I. Kozliak, Prepr. ACS Div. Petrol. Chem. 41 (1996) 628.
[39] A.J. Gordon, R.A. Ford, The Chemists Companion, J. Wiley and Sons, New York, 1972, p. 512.
[40] M.J. Stillman, A.J. Thomson, J. Chem. Soc., Faraday Trans. II (1974) 790.
[41] P.C. Minor, M. Gouterman, A.B.P. Lever, Inorg. Chem. 24 (1985) 1894.
[42] J. Mack, M.J. Stillman, Inorg. Chem. 36 (1997) 413.
[43] P. Day, P.A. O'Hill, M.G. Price, J. Chem. Soc. A (1968) 90.
[44] A.E. Martel, R.M. Smith, Critical Stability Constants, vol. 3, Plenum, New York, 1977, p. 356.